EVALUATING THE IMPACT OF SOLID MICRONEEDLES ON THE TRANSDERMAL DRUG DELIVERY SYSTEM FOR Ɏ-ORYZANOL

BHUPINDER KAUR[1]* , NISHANT THAKUR[1], MANISH GOSWAMI[2]

[1]Department of Pharmaceutics, University Institute of Pharma Sciences, Chandigarh University, Gharuan, Mohali, Punjab, India,
[2]Saraswati Group of Colleges, Gharuan, Mohali, Punjab, India
Email: bhupinder21990@gmail.com

ABSTRACT

Objective: This study's goals were to develop a minimally invasive array of biocompatible polymeric solid microneedles and formulate a transdermal patch of drug Ɏ-Oryzanol as per poke and patch technology.

Methods: Scanning electron microscopy was used to analyse the morphology of the solid microneedle arrays, which were created using a stereolithography (SLA) printer with high-resolution capabilities (25 and 140 microns for the z and x axes, respectively). Transdermal Patches of Ɏ-Oryzanol were formulated and evaluated for various characterization parameters. Further, the produced microneedle-transdermal drug delivery system of Ɏ-Oryzanol was examined for microneedle insertion skin and permeation of the drug across the porcine skin.

Results: Solid microneedle arrays were manufactured using biocompatible Class I Dental SG resin having dimensions of 600 μm height and 300 μm width with tip diameters of 30 μm and 1.85 mm interspacing (Distance from tip to tip) and they were strong enough to penetrate porcine skin to a depth of 381.356 μm crossing the stratum corneum layer without causing any structural changes. Transdermal patches containing Ɏ-Oryzanol were formulated using different ratios of HPMC: Eudragit E-100. Good, consistent, and transparent films were formulated when the thickness of the film ranges between 0.516±0.25-0.628±0.21 mm, average weights ranged from 168.23±2.61to171.22±1.25(10/cm²), folding endurance ranged in between 10 folds to 12 folds for all the formulations with tensile strength lie between the 0.365 kg/mm² to 0.465 kg/mm². All the formulations showed good drug content between 99.3±0.06%-90.4±1.64% with 100% flat surfaces. Moisture content was found in the range of 2.012±0.013 to 4.213±0.031. Drug permeation studies reveal that compound Ɏ-Oryzanol transdermal patches didn't show significant permeation across porcine skin (4.802.25 g/cm²) without piercing with microneedles while after poking skin using microneedles (74.502.35 g/cm²) drug showed good penetration properties. It was found that the amount of drug delivered increased to 44.251.57 g/cm² at 2 min, which was 14.502.35 g/cm² at 1 min to 4 min 74.502.35 g/cm².

Conclusion: Successful preparation of the Microneedle-Transdermal drug delivery system of Ɏ-Oryzanol and their evaluation indicated that the quality and consistency of the formulated preparation were excellent. With advantages in terms of lowered dose frequency, better patient compliance, and bioavailability, this may find use in the therapeutic field.

Keywords: Microneedles, 3D printing, Dental SG, Porcine skin, Permeation, Ɏ-Oryzanol, Transdermal patches

INTRODUCTION

Transdermal drug delivery (TDD) is the practice of administering medications to the bloodstream or nearby tissues through the skin [1, 2]. Transdermal pharmaceutical delivery is useful because it provides simple application, rapid dosage form removal, enhanced patient compliance (painless administration), and the capacity to adjust the rate of drug release [3, 4]. With this mode of delivery, the "hepatic first-pass effect" is also avoided because drug absorption is unaffected by variables such as pH, drug-food interaction, and enzyme activity [5]. The TDD approach does, however, have many serious drawbacks. This technique of administration is only appropriate for powerful lipophilic drugs since the skin's barrier function prevents the entry of polar hydrophilic drug molecules. Age of the skin, the location of application, and any pre-existing skin problems all have an impact on drug penetration [1]. Transdermal drug delivery has significantly advanced recently, making it possible to quickly transport hydrophilic polar medicinal substances into the body. One such illustration is the Microneedle-based TDDS, which is intended to alter the barrier function by rupturing the skin's outer layer and allowing hydrophilic molecules to enter the bloodstream [2]. The needles' length should be such that they can pass through the dermis without stimulating the dermal nerves [6, 7]. Drug-delivery microneedles are made of silicon, metal, ceramics, polymers, or other materials. Microneedles are made using a variety of methods [8–10]. These include micromolding with ceramics, silicon, or polydimethylsiloxane as the template-forming materials, lithography at a material's glass light transition, light with a twisted spin (metallic microneedles) and the method of blowing air with droplets. One of the following procedures is used to deliver transdermal drugs using microneedles. Inserting a patch after a blank microneedle is applied to the skin, a micro-needled medicated polymeric patch, or a metallic needle that has been coated in a medication solution.

This method is appropriate for the systemic administration of pharmacological compounds with high molecular weights and high-water solubilities [11-13]. Oliver, also known as Ɏ-Oryzanol, is derived from rice bran and rice bran oil, with the former containing a higher percentage of oliver (20–30%) than the latter [14-16]. Alpha-tocopherol, ascorbyl palmitate, and Ɏ-Oryzanol are used as antioxidants in quantities ranging from 0.2-2.5% [17-19]. Furthermore, Ɏ-Oryzanol blocks UVA and UVB radiation. For emulsions and hair care products, *oryzanol* serves as a stabilising, UV-absorbing, and additional antistatic agent [20–22]. Transdermal drug administration using microneedles may deliver a higher dosage without interfering with daily activities. In this research, solid microneedle patches containing Ɏ-Oryzanol were created, and the impact of microneedles on drug permeability was assessed. Utilizing HPMC and Eudragit E-100, patch formulations with or without microneedles were created, and porcine skin was used for drug penetration tests [23–25].

MATERIALS AND METHODS

Materials

Reagents and chemicals

Ɏ-Oryzanol was provided by Ricela Health Foods Ltd., Dhuri (Punjab)–India. Eudragit RLPO, Eudragit E100 and Eudragit L100, HPMC, Sodium carboxymethylcellulose and Carbopol 934 were

purchased from Yarrow chem India ltd. All the chemicals used in the study were of analytical grade.

Methods

Furnishing of the CADD design for fabrication of microneedles

Initially, the shape and orientation of the microneedle array were selected as pyramid and cone and were plotted on a 2D Template using the engineering software Solidworks has cross sections that are square and round, respectively [3]. All microneedles were 600 μm in length, with 300 μm for the base cross sections and 30 μm for the tip, separated by 1.85 mm (measured from tip-to-tip). The Microneedles were constructed with patches of an 11*11 array affixed to a solid 15x15x1 mm substrate [30, 31]. Further, this array was examined and verified with the given literature and this array was drafted in a CAD. stl file using AutoCAD; Autodesk, Cupertino, CA, USA. The 3D fig. of the design of Microneedles is shown in fig. 1

Fig. 1: 3D microneedles array

Development of microneedle array

Form Labs' Dental SG biocompatible Class I resin was chosen as the printing material. The stereolithography (SLA) printer, used by Adroitec Pvt. Ltd. to manufacture the arrays, offers high-resolution capabilities (25 and 140 microns for z and x axes, respectively).

Formulation of transdermal patches

Transdermal patches containing ɣ-*Oryzanol* were produced utilising the solvent casting method in a glass mould built locally. The most effective mixtures of polymer, plasticizer, and solvent were tested using placebo patches [32]. Using a magnetic stirrer, the best polymers, Eudragit E-100 and HPMC, were mixed to weigh 500 mg and were then dissolved in 10 ml of an isopropanol-dichloromethane (60:40) solvent mixture. The drug solution was gradually added to the polymer solution and thoroughly mixed to produce a homogenous solution. Di-n-butyl phthalate, which made up 30% of the weight of the polymer, was utilised as a plasticizer [24, 35]. Different polymer ratios were tried to formulate patches as mentioned in table 1. Further, the formulated transdermal patches were evaluated for various characterization tests.

Characterization studies

Investigation of drug-polymer compatibility

A Perkin Elmer FTIR spectrophotometer (RXIFT-IR system) was used to test the Fourier transform infrared spectroscopy (FTIR) of ɣ-*Oryzanol* and blends of drug with Eudragit-E100 and HPMC to assess drug-polymer compatibility [34]. After the sample had been exposed to potassium bromide, data was collected spanning the spectral range of 450 to 4000 cm^{-1}.

Table 1: Formulation variables for transdermal patches

Code	HPMC (mg)	Eudragit E-100 (mg)	IPA (ml)	DCM (ml)	Di-n-butyl phthalate (%)	Drug (mg)
ORZ-1	0	50	60	40	30	25
ORZ-2	5	0	60	40	30	25
ORZ-3	30	20	60	40	30	25
ORZ-4	20	30	60	40	30	25
ORZ-5	40	10	60	40	30	25
ORZ-6	10	40	60	40	30	25

Scanning electron microscopy (SEM)

With a low accelerating voltage, SEM (Hitachi SU 8030, Japan) was used to examine the morphology of microneedle patches to determine the size, shape, and other physical characteristics of the needles (1.0kV) [24, 25]. To prevent electrical charges on the cross microneedles, a modest accelerating voltage was applied [17-19]. Digital photographs of coated cross-microneedles were taken at various magnifications from a fixed working distance (11.6 mm) (30, 80, 110 or 120 x).

Thickness and Weight variation folding of formulated transdermal patches

Using a Vernier calliper, prepared microneedle patches and transdermal patches were evaluated for thickness uniformity [17, 18]. Individually weighing patches that were chosen at random allowed for the study of weight variance, and micrometer measurements of film thickness were made at random locations on all batches of the film [26].

Drug content determination

To extract the drug from the transdermal patch, a 1 cm^2 transdermal patch containing 25 mg of the drug was dissolved in phosphate buffer pH 8 (60%), isopropyl alcohol (40%) and labrasol (0.5%) and agitated continuously for 24 h using a magnetic stirrer. The amount of drug present was determined spectrophotometrically at a wavelength of 325 nm following filtration and dilution using phosphate buffer [26, 27].

Flatness

To ensure that the created transdermal patches have a smooth surface and won't contract over time, a flatness study was carried out. The film was divided into three longitudinal strips, each cut at a separate location. Each strip's length was measured, along with the variation in length due to non-uniformity in flatness, using a percent constriction scale where 0% constriction is equal to 100% flatness. The formula for percent constriction was $(L_1-L_2)/l_1* 100$. Here, each strip has a beginning length of L_1 and a final length of L_2. [26-28].

Tensile strength and folding endurance

The folding endurance rating was determined by how many times the film could be folded in the same location without breaking [37]. The weight pulley method was used to calculate tensile strength [29].

Moisture content and uptake

To determine the percentage of moisture content and uptake, produced films were weighed separately and maintained in desiccators containing activated calcium chloride or saturated potassium chloride solutions for 24 h, respectively [26].

Skin permeation studies for ɣ-*Oryzanol*

In a nearby abattoir, porcine ears were collected from recently slaughtered pigs. Full-thickness, non-dermatomed skin was chosen, and the outer layer that was intended to be used for the experiment was separated using a skin grafting handle after being washed with ice-cold, deionized water [18, 19]. A slice of skin with a uniform thickness of 1 mm was put on the Franz diffusion cell as depicted in fig. 2. The drug's additional flux and permeability coefficient were calculated from the permeation studies. Because pig skin has similar permeability qualities to human skin, it was employed in skin

permeation investigations. Since it is technically more challenging to get undamaged split-thickness skin, the general rule with pig skin in

dermal absorption, specifically for the research of cosmetic components, is whole-thickness skin.

Fig. 2: Preparation of porcine skin samples and mounting on modified franz diffusion assembly

Permeation of Ɣ-*Oryzanol* across porcine ear skin was calculated using the Modified Franz diffusion cell apparatus**.** The volume of the donor compartment present in the test apparatus was found to be 3.319 cm³ and the area was calculated which came to be around 1.3263 cm². Phosphate buffer pH 8 (60%), Iso-Propyl alcohol (40%) and Labrasol (0.5%) were used as receptor media and the temperature of this media was maintained at 37.5 ℃ throughout the studies with water circulation and stirring at fixed RMP [31].

A completely saturated solution of Ɣ-*Oryzanol* i.e., 100% was prepared in the above-said media and it was placed over the skin surface in the donor compartment, which was further sealed from the atmospheric interference by parafilm. At different time intervals of 0 h, 1h, 2h, 3h up to 24 h, 1 ml of aliquots were taken from the receptor compartment to access the permeability of the drug across the skin. Each withdrawn aliquot was replaced by an equal volume of media in the receptor [33]. Subsequently, more of the dilutions of Ɣ-*Oryzanol* were prepared in the range of 10%, 20%, 30%, 40%, 50%, 60%, 70%, 80%, 90% and all the results were taken in triplicate to meet the statistical requirements.

Skin permeation studies by microneedle treatment

In a nearby abattoir, porcine ears were harvested from recently slaughtered pigs. At first, tap water was used to wash the ears, and soft paper was used to dry them. Using an ordinary shaving blade, hair was eliminated. To obtain whole-skin samples, ears were sectioned using a skin grafting handle. Samples of skin were sliced into circles [31-33]. Full-thickness skin samples were laid over support made of polystyrene foam, with the stratum corneum on top. Manual pressure was used to apply microneedle arrays to the centre of skin samples. Before each re-insertion, arrays were rotated by around 90 degrees for repeated insertions.

A portion of skin with a uniform thickness of 1 mm was put on the Franz diffusion cell. The drug's additional flux and permeability coefficient were calculated from the permeation studies.

Permeation of Ɣ-*Oryzanol* across porcine ear skin was calculated using the Modified Franz diffusion cell apparatus**.** The volume of the donor compartment present in the test apparatus was found to be 3.319 cm³ and the area was calculated which came to be around 1.3263 cm². Phosphate buffer pH 8 (60%), Iso-Propyl alcohol (40%) and Labrasol (0.5%) were used as receptor media and the temperature of this media was maintained at 37.5 ℃ throughout the studies with water circulation and stirring at fixed RMP [26, 27].

A completely saturated solution of Ɣ-*Oryzanol* i.e., 100% was prepared in the above-said media and it was placed over the skin surface in the donor compartment, which was further sealed from

the atmospheric interference by parafilm. At different time intervals of 0 h, 1h, 2h, 3h up to 24 h, 1 ml of aliquots were taken from the receptor compartment to access the permeability of the drug across the skin. Each withdrawn aliquot was replaced by an equal volume of media in the receptor. Subsequently, more of the dilutions of Ɣ-*Oryzanol* were prepared in the range of 10%, 20%, 30%, 40%, 50%, 60%, 70%, 80%, 90% and all the results were taken in triplicate to meet the statistical requirements.

Penetration of microneedles in porcine skin

Pig-ear skin that was quickly gathered after pigs were slain at a nearby slaughterhouse was used for *in vitro* skin insertion research. Damaged skin was scraped from skin samples after they had been cleansed with cold water. The entire skin was meticulously separated from the underlying cartilage to generate full-thickness skin membranes. The skin was defrosted and sliced into 2*2 cm squares before the diffusion tests. Thumbtacks were used to secure the skin samples into a firm framework before the microneedle arrays adhered to their surface. The skin was physically compressed with microneedles for 30 seconds with force comparable to pressing an elevator button or a stamp into an envelope; then, the compression site was peeled off and exposed to a fluorescent dye for 1 minute. Skin samples that were treated for histological analysis had the remaining dye removed. Skin samples were fixed in 10% formalin, dried, and embedded in paraffin to create histology specimens [29]. To evaluate penetration depth, skin samples were stained with methylene blue dye and examined under an Olympus fluorescence microscope as shown in fig. 10.

RESULTS AND DISCUSSION

The additive manufacturing process of stereolithography was successfully used to create MN arrays with needles in the shapes of cones and pyramids. Using computer-aided design (CAD) models as a starting point, the SLA builds structures layer by layer using a Class I biocompatible resin. One of the few commercially available, FDA-certified polymers that are both compatible with stereolithography printers and a Class I polymer that is compatible with Form 2 technology Dental SG resin. Fig. 3 depicts the MN patches that SLA produced. Due to the low cost of the printing material and the speed at which items can be manufactured, SLA is a popular technology for MN fabrication. Quantitatively speaking, the commercial SLA machines currently available have a restricted print volume, although with the present print volume (145*145*175 mm), up to 49 MN arrays can be produced in 2 h using the suggested dimensions and procedure. Printers with higher print volumes must be introduced to scale the technique up on an industrial scale. Parallel printing in several printers, however, may swiftly and

accurately manufacture a huge number of arrays due to the low cost of these printers and the speed of fabrication.
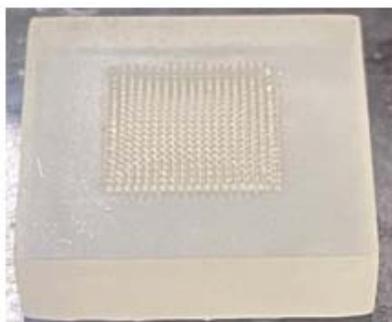

Fig. 3: Fabricated microneedles

FTIR spectroscopic study analysis

ɣ-*Oryzanol* shows C=O stretching at 1684 cm^{-1}. Further, alkenyl C=C stretch, aromatic ring stretch, and primary amine stretch confirms the purity and structure of ɣ-*Oryzanol*. In Eudragit E-100 ester C = O stretching peak was detected at 1722.48 cm^{-1} while C-H Stretch was at 2955 cm^{-1}. Hydrocarbon chain vibrations were found at 1385, 1450–1490 and 2950 cm^{-1}. C-O Stretch was observed at 1150 cm^{-1}. In the IR graph of HPMC, the identification of peak at 3465 cm^{-1} shows the presence of-OH groups and the peak at 2901 cm^{-1} shows the presence of C-H stretch. FTIR of ɣ-*Oryzanol* and ɣ-*Oryzanol* with Eudragit and HPMC (fig. 4,5,6) suggested that there was no chemical interaction between the drug and excipients used. Peak area changes could arise from simple component mixing alone, with no evidence of chemical interaction.
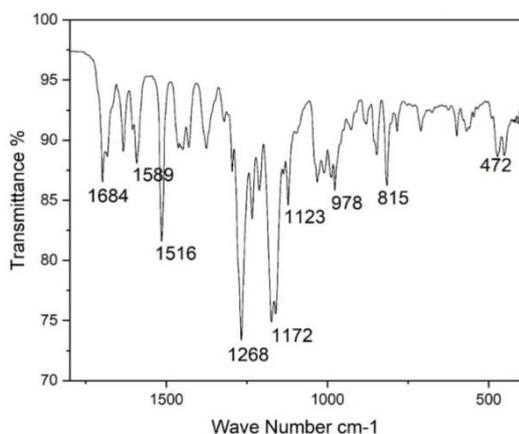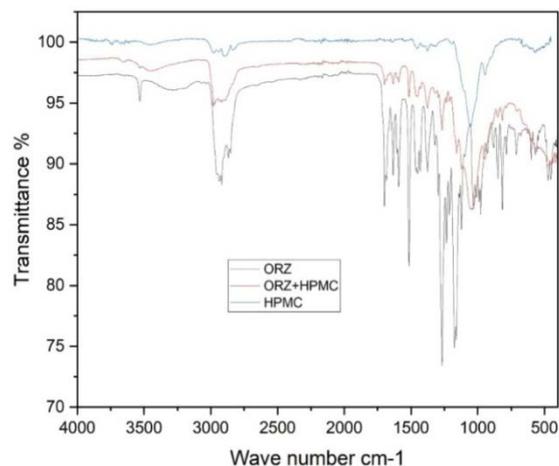

Fig. 4: FTIR spectra of ɣ-*Oryzanol*

Fig. 5: FTIR spectra of ɣ-*Oryzanol* and HPMC
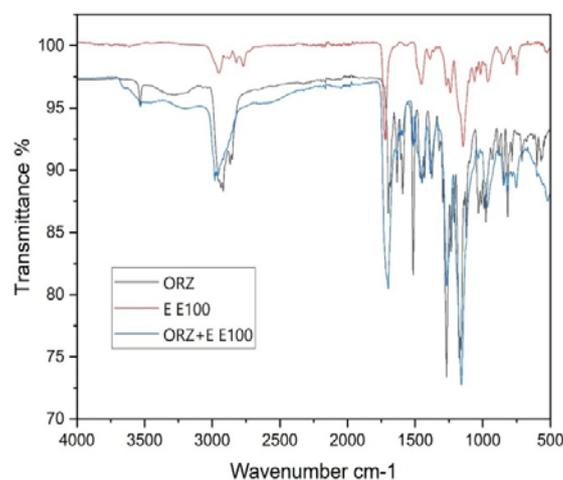

Fig. 6: FTIR spectra of ɣ-*Oryzanol* and Eudragit E-100

SEM analysis of fabricated microneedles

Fabricated microneedles were studied under the scanning electron microscope. SEM studies confirm that each microneedle has dimensions approx. 600 μm height and 300 μm width with tip diameter of 30 μm and 1.85 mm interspacing (Distance from tip to tip) as shown in fig. 7. Sharp needle tips that are better for implantation into the skin were produced as a result of the printer's high resolution making it feasible to repeatedly manufacture very detailed arrays.
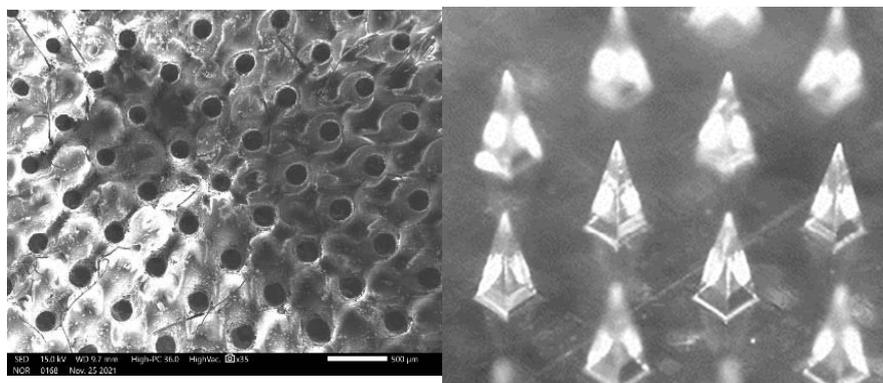

Fig. 7: SEM image of prepared microneedles

Evaluation of films

Good, consistent, and transparent films were created by combining HPMC and Eudragit E-100. Without plasticizers, they were found to be fragile. Then, to create films with good elasticity as reported in earlier experiments, dibutyl phthalate was added as a plasticizer to reduce the brittleness [24, 36].

A micrometer was used to measure the thickness of the films, which consistently ranged between 0.516±0.25 for ORZ-3 to 0.628±0.21 mm for ORZ-5. From these values, it was quite clear that with an increase in the concentration of Eudragit E-100 thickness of the patch increases. It implies that the use of a suitable polymer is a precondition for producing a patch of optimal thickness, failure to which may retard the release of medicine from the patch. The average weights ranged from 168.23±2.61 to 171.22±1.25 (10/cm^2), showing that different batches' weights were often comparable. The folding endurance was discovered to be greater than 11, so it was clear that the prepared patches had both the flexibility and strength

to sustain mechanical strain. The formulations which comprise HPMC were found to have high values of folding endurance. All the formulations showed good drug content; however, highest drug content was observed with ORZ-4 showing about 99.3±0.06% while the lowest was observed in ORZ-2, having a value 90.4±1.64%. All the prepared patches were smooth in appearance and there was no eruption; hence 100% flatness of the surface was observed. The results showed that the method used to make the patches were able to produce patches with a consistent drug content and little patch variability. The results of tests on tensile strength and folding endurance showed that the patches would not fracture and would maintain their integrity under typical skin folding. Tensile strength was found in the range of 0.332±0.03 to 0.465±0.04 for all the formulations, which further confirms the uniformity of transdermal patches. Moisture content present between all the patches shows variability in the range of 2.012±0.013 to 4.213±0.031 being highest in ORZ-4 and lowest in ORZ-1. The results of the physicochemical characterization of patches are shown in table 2.

Table 2: Physicochemical characterization of transdermal patches

Code	The ratio of E-100: HPMC	Average weight (10/cm^2)	Thickness (mm)	Drug content (%)	Folding Endurance	Flatness (%)	Tensile strength (kg/mm^2)	Moisture content (%)
ORZ-1	0:5	169.02±1.05	0.568±0.02	91.3±2.14	12±2.14	100±0	0.365±0.04	2.012±0.013
ORZ-2	5:0	170.12±2.23	0.611±0.05	90.4±1.64	11±1.14	100±0	0.415±0.01	2.112±0.022
ORZ-3	3:2	168.23±2.61	0.516±0.25	91.5±0.14	10±2.52	100±0	0.412±0.02	3.021±0.014
ORZ-4	2:3	169.55±2.05	0.618±0.05	99.3±0.06	12±1.12	100±0	0.332±0.03	4.213±0.031
ORZ-5	4:1	171.22±1.25	0.628±0.21	97.1±0.24	10±1.13	100±0	0.465±0.04	3.752±0.002
ORZ-6	1:4	173.09±2.25	0.625±0.05	95.3±1.14	12±0.23	100±0	0.457±0.01	2.523±0.011

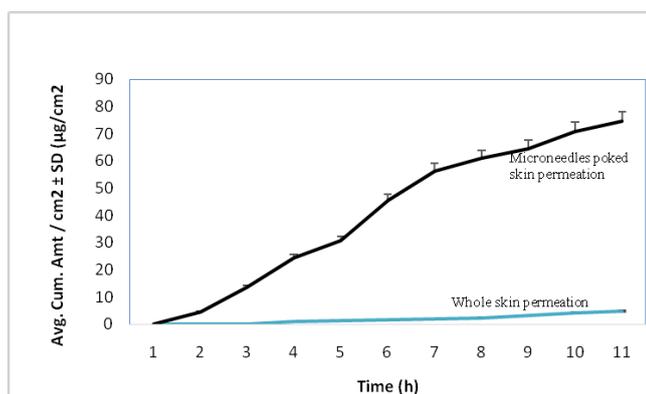(n=3, mean±SD; experiments were conducted in triplicate)

Fig. 8: *In vitro* permeation profile of *Ɣ-Oryzanol* through microneedle-treated porcine ear skin (n=3, mean±SD)

Formulation ORZ1 having Eudragit E-100: HPMC ratio of 0:5 showed minimum release; however, formulation ORZ 4 with a polymer ratio of 2:3 had the maximum release. The increase in the release in the formulation ORZ 4 can be attributed to the increased retention time and enhanced dissolution. However, there is no significant difference in the concentration of polymers in the formulation, but the optimum concentration of the HPMC and Eudragit increased the drug wetting time and dissolution.

Penetration of MN in porcine skin

Using a texture analyser, the fabricated array MNs were implanted into samples of pig skin. None of the MN designs failed to penetrate the skin; they all succeeded. Throughout the penetration, force against displacement data was continuously recorded. The microneedles were strong enough to penetrate porcine skin to a depth of 381.356 μm crossing the stratum corneum layer without fracturing or causing any structural changes.

***In vitro* permeation studies using vertical Franz diffusion cells**

Using dermatomed porcine ear skin, the impact of different needle lengths, equilibration times, and treatment lengths on *Ɣ-Oryzanol*

permeation was assessed *in vitro*. Control skin was chosen since it had neither been equilibrated nor punctured by microneedles. The passive diffusion experiments were carried out with the assumption that no *Ɣ-Oryzanol* would permeate the skin. Plotting the amount of *Ɣ-Oryzanol* that spread across the skin after being subjected to various treatments as a function of time (n=3) is shown in fig. 8.

In contrast to whole skin permeation, which was determined to be (4.802.25 g/cm^2), solid microneedle therapy (74.502.35 g/cm^2) delivered a substantially higher amount of medication to the receptor. The majority of medication molecules entered the body through micropores as opposed to the skin covering the channels. The highest amount of medication delivered via solid microneedle treatment was rationally supported by these characterization results. Longer microneedles have the potential to cause more discomfort and damage to the small blood capillaries, which could lead to bleeding since they are more likely to get to the nerve fibres [23]. Additionally, because of the larger surface area of channels, bacteria or other foreign materials may be able to enter the skin tissues. A study using full-thickness porcine ear skin revealed that little *Ɣ-Oryzanol* was delivered to the receptor chamber and that the majority of it remained in the stratum corneum. As a result, the

amount of drug that was absorbed through the skin was the same in the dermatoming group as it was in the control group (4.802.25 g/cm²). Plotted in fig. 9 (n=3) is the impact of various solid microneedle treatment times (1, 2, and 4 min) on transdermal delivery of *Ɣ-Oryzanol*. It was found that the amount of drug delivered increased negligibly when the needle insertion time was increased from 1 to 2 min. Although the drug release was found to be (44.251.57 g/cm²) at 2 min, there was a considerable improvement in drug permeation when the treatment time was increased from 1 min

(14.502.35 g/cm²) to 4 min (74.502.35 g/cm²). Therefore, among the various trials, the 4-min treatment duration delivered the most drug. Li *et al.* explanation's that the skin contracts quickly and microchannels close quickly during shorter treatment durations resulting in lesser skin permeability [38]. Longer treatment times result in reversible plastic deformation, a delay in elasticity recovery, a longer channel survival time, and a considerable increase in skin permeability in the skin around the channels.
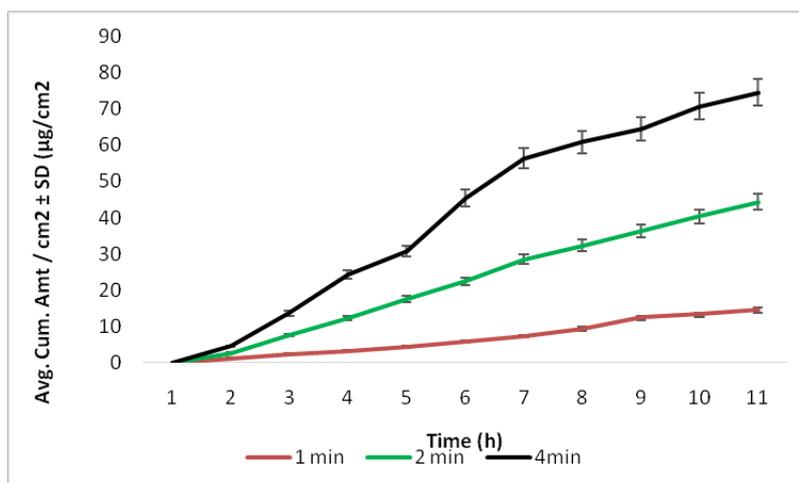

Fig. 9: *In vitro* permeation profile of *Ɣ-Oryzanol* through microneedle-treated porcine ear skin: Solid-MN 1 min, Solid-MN 2 min, and solid-MN 4 min (n=3, mean±SD)

Fig. 10: Microscopic Image of pierced porcine skin using fabricated microneedles observed at 40X

CONCLUSION

This study was built using a comparison of the design, strength under stress, and material used to create a microneedle that can meet the criterion to pierce human skin while preventing harm to the skin and the needle itself.

The results of the current investigation showed that micro needling improved the transdermal distribution of *Ɣ-Oryzanol* over dermatomed porcine ear skin. The needle length, micro-needling, and microneedle treatment period all had an impact on the variation in the *in vitro* drug permeation profile. The geometry and size of microneedles were described using scanning electron microscopy. The mean cumulative amount of medication that was absorbed through the skin at 24 h in the *in vitro* permeation trials using solid microneedles was significantly higher than that of untreated whole skin samples.

ABBREVIATIONS

MN-Microneedles, TDD-Transdermal drug delivery

FUNDING

AUTHORS CONTRIBUTIONS

All the authors have contributed equally.

CONFLICT OF INTERESTS

Declared none

REFERENCES

1. Hao Y, Li W, Zhou XL, Yang F, Qian ZY. Microneedles-based transdermal drug delivery systems: a review. J Biomed Nanotechnol. 2017;13(12):1581-97. doi: 10.1166/jbn.2017.2474, PMID 29490749.
2. Anantrao JH, Nath PA, Nivrutti PR. Drug penetration enhancement techniques in transdermal drug delivery system: a review. J Pharm Res Int. 2021;33(19B):46-61. doi: 10.9734/jpri/2021/v33i19B31337.
3. Nagadev C, Rao MDS, Venkatesh P, Hepcykalarani D, Prema R. A review on transdermal drug delivery systems. Asian J Res Pharm Sci. 2020;10(2):109-14. doi: 10.5958/2231-5659.2020.00021.1.
4. Gaikwad AK. Transdermal drug delivery system: formulation aspects and evaluation. Compr J PharmSci. 2013;1(1):1-10.
5. Mali AD, Bathe R, Patil M. An updated review on transdermal drug delivery systems. Int J of Adv in Sci Res. 2015;1(6):244-5. doi: 10.7439/ijasr.v1i6.2243.

6. Sarkar P, Das S, Majee SB. Biphasic dissolution model: a novel strategy for developing discriminatory *in vivo* predictive dissolution model for BCS class ii drugs. Int J Pharm Pharm Sci. 2022;14(4):20-7. doi: 10.22159/ijpps.2022v14i4.44042.

7. Ghosh M. Review on recent trends in rice bran oil processing. J Amer Oil Chem Soc. 2007;84(4):315-24. doi: 10.1007/s11746-007-1047-3.

8. Filho Acva GMIF, Duarte SF, Lima-Neto ABM. Gamma-oryzanol has equivalent efficacy as a lipid-lowering agent compared to fibrate and statin in two dyslipidemia mice models. Int J Pharm Pharm Sci. 2014;6(11):61-4.

9. Manoj VR, Manoj H. Review on transdermal microneedle-based drug delivery. Asian J Pharm Clin Res. 2019;12(1):18-29. doi: 10.22159/ajpcr.2019.v12i1.27434.

10. Kalona PA, Sundaresan U, Kasinathan ID, Muthiah C. Studies on red rice bran and its health benefits of food application-a review. Int J Pharm Res. 2020;14(3):1-6.

11. Sen S, Chakraborty R, Kalita P. Rice–not just a staple food: A comprehensive review on its phytochemicals and therapeutic potential. Trends Food Sci Technol. 2020;97:265-85. doi: 10.1016/j.tifs.2020.01.022.

12. Banerjee N, Chatterjee S, Bhattacharjee S, Bhattacharya BDES, Mukherjee S. Rice bran oil consumption: cardiovascular disease and obesity risk reduction. Drug Invent Today. 2018;10(1):402-7.

13. Panda A, Matadh VA, Suresh S, Shivakumar HN, Murthy SN. Non-dermal applications of microneedle drug delivery systems. Drug Deliv Transl Res. 2022;12(1):67-78. doi: 10.1007/s13346-021-00922-9, PMID 33629222.

14. Agrawal S, Gandhi SN, Gurjar P, Saraswathy N. Microneedles: an advancement to transdermal drug delivery system approach. J App Pharm Sci. 2020;10(3):149-59. doi: 10.7324/JAPS.2020.103019.

15. Dukare MV, Saudagar RB. Needle-free injection system. Int J Curr Pharm Sci. 2018;10(2):17-24. doi: 10.22159/ijcpr.2018v10i2.25885.

16. Vora LK, Moffatt K, Tekko IA, Paredes AJ, Volpe Zanutto F, Mishra D. Microneedle array systems for long-acting drug delivery. Eur J Pharm Biopharm. 2021;159:44-76. doi: 10.1016/j.ejpb.2020.12.006, PMID 33359666.

17. SR, DS, IH. Microneedle drug delivery system-overview. Int J Res Pharm Sci. 2011;109:1249-58.

18. Zong Q, Guo R, Dong N, Ling G, Zhang P. Design and development of insulin microneedles for diabetes treatment. Drug Deliv Transl Res. 2022;12(5):973-80. doi: 10.1007/s13346-021-00981-y, PMID 33851362.

19. Meng F, Hasan A, Mahdi Nejadi Babadaei M, Hashemi Kani P, Jouya Talaei A, Sharifi M, Cai T, Falahati M, Cai Y. Polymeric-based microneedle arrays as potential platforms in the development of drugs delivery systems. J Adv Res. 2020;26:137-47.

20. Damiri F, Kommineni N, Ebhodaghe SO, Bulusu R, Jyothi VGSS, Sayed AA. Microneedle-based natural polysaccharide for drug delivery systems (DDS): progress and challenges. Pharmaceuticals (Basel). 2022;15(2):190. doi: 10.3390/ph15020190, PMID 35215302.

21. Sabri AH, Ogilvie J, hamid AK, Shpadaruk V, McKenna J, Segal J, Scurr DJ, Marlow M. Expanding the applications of microneedles in dermatology. Eur J Pharm Biopharm. 2019; 140:121-40.

22. He X, Sun J, Zhuang J, Xu H, Liu Y, Wu D. Microneedle system for transdermal drug and vaccine delivery: devices, safety, and prospects. Dose-Response. 2019 Oct 14;17(4):1559325819878585. doi: 10.1177/1559325819878585, PMID 31662709.

23. Parhi R, N DS. Review of microneedle-based transdermal drug delivery systems. PCI- Approved-IJPSN 2019;12(3):4511-23. doi: 10.37285/ijpsn.2019.12.3.1.

24. Sharma C, Thakur N, Kaur B, Goswami M. Investigating effects of permeation enhancers on percutaneous absorption of loxapine succinate. Int J Appl Pharm. 2022;14(4):158-62. doi: 10.22159/ijap.2022v14i4.44896.

25. Lahiji SF, Dangol M, Jung H. A patchless dissolving microneedle delivery system enabling rapid and efficient transdermal drug delivery. Sci Rep. 2015;5:7914. doi: 10.1038/srep07914, PMID 25604728.

26. Dharadhar S, Majumdar A, Dhoble S, Patravale V. Microneedles for transdermal drug delivery: a systematic review. Drug Dev Ind Pharm. 2019 Feb;45(2):188-201. doi: 10.1080/03639045.2018.1539497, PMID 30348022.

27. Prajapati ST, Patel CG, Patel CN. Formulation and evaluation of transdermal patch of repaglinide. ISRN Pharm. 2011;2011:651909. doi: 10.5402/2011/651909, PMID 22389856.

28. Kozuka C, Kaname T, Shimizu Okabe C, Takayama C, Tsutsui M, Matsushita M. Impact of brown rice-specific γ-oryzanolon epigenetic modulation of dopamine D2 receptors in brain striatum in high-fat-diet-induced obesity in mice. Diabetologia. 2017 Aug;60(8):1502-11. doi: 10.1007/s00125-017-4305-4, PMID 28528402.

29. Ramadon D, McCrudden MTC, Courtenay AJ, Donnelly RF. Enhancement strategies for transdermal drug delivery systems: current trends and applications. Drug Deliv Transl Res. 2022 Apr;12(4):758-91. doi: 10.1007/s13346-021-00909-6, PMID 33474709.

30. Xu J, Xu D, Xuan X, He H. Advances of microneedles in biomedical applications. Molecules. 2021 Sep 29;26(19):5912. doi: 10.3390/molecules26195912, PMID 34641460.

31. Damiri F, Kommineni N, Ebhodaghe SO, Bulusu R, Jyothi VGSS, Sayed AA. Microneedle-based natural polysaccharide for drug delivery systems (DDS): progress and challenges. Pharmaceuticals (Basel). 2022 Feb 3;15(2):190. doi: 10.3390/ph15020190, PMID 35215302.

32. Das A, Ahmed AB. Formulation and evaluation of transdermal patch of indomethacin containing patchouli oil as a natural penetration enhancer. Asian J Pharm Clin Res. 2017 Nov 1;10(11):320-5. doi: 10.22159/ajpcr.2017.v10i11.20926.

33. Chaiyasan W, Srinivas SP, Niamprem P, Tiyaboonchai W. Penetration of hydrophilic sulforhodamine B across the porcine cornea ex-vivo. Int J Appl Pharm. 2018;10(6):94-102. doi: 10.22159/ijap.2018v10i6.28505.

34. Thakur N, Kaur B, Goswami M, Sharma C. Compatibility studies of the thiocolchicoside with Eudragit RLPO, Eudragit E100 and Eudragit L100 using thermal and non-thermal methods. Drug Comb Ther. 2022;4(1):1. doi: 10.53388/DCT2021100301.

35. Sharma C, Thakur N, Kaur B, Goswami M. Transdermal patches: state of the art. Int J Drug Deliv Technol. 2020;10(3):414-20. doi: 10.25258/ijddt.10.3.19.

36. Zhan X, Mao Z, Chen S, Chen S, Wang L. Formulation and evaluation of transdermal drug-delivery system of isosorbide dinitrate. Braz J Pharm Sci. 2015;51(2):373-82. doi: 10.1590/S1984-82502015000200015.

37. Patel KN, Patel HK, Patel VA. Formulation and characterization of drug in adhesive transdermal patches of diclofenac acid. Int J Pharm Pharm Sci. 2012;4(1):296-9.

38. Milewski M, Yerramreddy TR, Ghosh P, Crooks PA, Stinchcomb AL. *In vitro* permeation of a pegylated naltrexone prodrug across microneedle-treated skin. J Control Release. 2010;146(1):37-44. doi: 10.1016/j.jconrel.2010.05.034, PMID 20678989.